ChemPubSoc Europe

DOI: 10.1002/cssc.201601154

CHEMSUSCHEM Full Papers

Glycidol: an Hydroxyl-Containing Epoxide Playing the Double Role of Substrate and Catalyst for CO_2 Cycloaddition Reactions

Francesco Della Monica,[a, b] Antonio Buonerba,[a, b] Alfonso Grassi,[a, b] Carmine Capacchione,*[a, b] and Stefano Milione[a, b]

Glycidol is converted into glycerol carbonate (GC) by coupling with CO_2 in the presence of tetrabutylammonium bromide (TBAB) under mild reaction conditions ($T = 60\,^{\circ}C$, $P_{CO_2} = 1$ MPa) in excellent yields (99%) and short reaction time ($t = 3$ h). The unusual reactivity of this substrate compared to other epoxides, such as propylene oxide, under the same reaction conditions is clearly related to the presence of a hydroxyl functionality on the oxirane ring. Density functional theory calculations (DFT) supported by ^{1}H NMR experiments reveal that the unique behavior of this substrate is a result of the formation of intermolecular hydrogen bonds into a dimeric structure, activating this molecule to nucleophilic attack, and allowing the formation of GC. Furthermore, the glycidol/TBAB catalytic system acts as an efficient organocatalyst for the cycloaddition of CO_2 to various oxiranes.

Introduction

The development of environmentally friendly chemical engineering is one of the key factors for global sustainability. This issue requires not only the development of processes following green-chemistry principles, but also the use of feedstocks from renewable resources. In such a context, the coupling of CO_2 with epoxides represents a very attractive reaction because of the possibility to recover waste through an atom-economical process with the production of value added products, such as cyclic carbonates.[1]

This reaction is catalyzed by many transition metal complexes.[1a,b] In the last years, with the aim to reduce the usage of potentially toxic or costly metals in the synthesis of cyclic carbonates, the attention has shifted to the use of organocatalysts.[2] As in the case of metal-based catalysts, the most effective systems contain two components: one component activates the substrate to the attack of the other component, the nucleophile, typically an ammonium or trisalkylphosphineiminium salt, KI or dimethylaminopyridine (DMAP), to achieve the formation of the desired cyclic carbonate.

Notably, in many cases the presence of hydrogen-bond donors, such as polyalcohols,[3] phenols or polyphenols,[4] carboxylic acids,[5] silanols,[6] chitosan,[7] cellulose,[8] β-cyclodextrin,[9] amino acids and amino alcohols[10] and graphene oxide,[11] plays a crucial role in determining the catalyst performance for the addition of CO_2 to oxiranes.

In the last decade, parallel to the development of CO_2 chemistry, the increasing production of biodiesel from vegetable oils has offered to the market a new cheap raw material: glycerol. The decrease of the glycerol price has triggered a growing interest not only in the new possible use of this product, but also in the development of processes for the efficient conversion of this molecule to valuable commodity chemicals in both academic and industrial environments.[12]

Among the possible glycerol derivatives, glycerol carbonate (GC) is a particularly interesting target because, owing to its physical properties, GC has potential application as low volatile organic compounds (VOCs), a bio-based alternative to organic solvents from a non-renewable resource. Furthermore, the presence in the GC skeleton of both a hydroxyl group and a 2-oxo-1,3-dioxolane group renders this molecule a major candidate as chemical intermediate for the synthesis of other value added products.[13]

Actually, the most covered routes from glycerol to glycerol carbonate involve the reaction of glycerol with phosgene or its transesterification with alkyl carbonates.[14] More recently, the direct carboxylation of glycerol[15] and the glycerolisys of urea[16] in the presence of heterogeneous catalysts were also achieved. Nevertheless these synthetic approaches often require the use of highly toxic ($COCl_2$) or highly inflammable reactants (CO), harsh reaction conditions and in many cases present a low selectivity to the desired product. A 100% atom-

[a] F. Della Monica, Dr. A. Buonerba, Prof. A. Grassi, Prof. C. Capacchione, Dr. S. Milione
Dipartimento di Chimica e Biologia "Adolfo Zambelli"
Università degli Studi di Salerno
via Giovanni Paolo II
84084 Fisciano, SA (Italy)
E-mail: ccapacchione@unisa.it

[b] F. Della Monica, Dr. A. Buonerba, Prof. A. Grassi, Prof. C. Capacchione, Dr. S. Milione
Interuniversity Consortium Chemical Reactivity and Catalysis (CIRCC)
via Celso Ulpiani 27
70126, BA (Italy)

Supporting Information and the ORCID identification number(s) for the author(s) of this article can be found under http://dx.doi.org/10.1002/cssc.201601154.

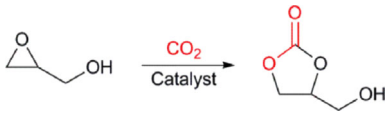

Scheme 1. Synthesis of glycerol carbonate (GC) from glycidol and CO_2.

economical and environmental friendly way to produce GC is the cycloaddition of CO_2 to glycidol (Scheme 1).

This reaction has been reported to be promoted by several catalytic systems based on transition metal complexes[17] and in some case on polyphenols as organocatalysts.[5b,e] Very recently a new and high efficient route for the production of glycidol from 2-chloro-1,3-propanediol, a by-product in the epichlorohydrin production plant, was reported offering an economical and feasible way to obtain glycidol.[18]

It is worth noting that differently to other epoxides, glycidol, owing to the presence of an hydroxyl functionality, can also act as hydrogen-bond donor. In other words, glycidol seems to be a non-innocent substrate with the possibility of playing the double role of reagent and catalyst.

Results and Discussion

In our ongoing search for active catalysts for the coupling of CO_2 with epoxides[17g–i] we have noticed that glycidol is sensibly more reactive than other epoxides [e.g., propylene oxide (PO)].

To get deeper insights into the reaction of glycidol with CO_2, we decided to investigate the reaction in the presence of bis(triphenylphosphine)iminium chloride and various ammonium salts. The main results, reported in Table 1, clearly show the efficient conversion (70–85%) of this substrate to the desired product under mild, solventless conditions ($T = 80\,^{\circ}C$, $P_{CO_2} = 1.0$ MPa). Among the promoters investigated (entry 1–4, Table 1), tetrabutylammonium bromide (TBAB) resulted the most efficient one. Noteworthy, the low TBAB loading (1 mol% of TBAB, entry 4) and the reaction time required ($t = 1$ h) for the high conversion (85%) of the substrate are by far more favorable than those reported for other ammonium salts with conventional epoxides, such as PO and cyclohexeneoxide (CHO).[19] When the reaction temperature was decreased below 60 °C, the epoxide conversion was negligible under the same reaction conditions (entries 6 and 7, Table 1). On the other hand, by increasing the TBAB loading to 5%, it is possible to reach the complete conversion (>99%) in only 3 h at 60 °C. Notably a good conversion to GC is still possible under very mild reaction conditions (40 °C, $P_{CO_2} = 0.1$ MPa, entry 12, Table 1). For comparison, methylglycidyl ether (entry 13, Table 1) and PO (entry 14, Table 1) yielded a much lower conversion.

With the aim to shed more light on the mechanism underlying the facile conversion of glycidol to GC, the reaction path was investigated by density functional theory (DFT) calculations. According to the previous DFT studies on the cycloaddition reaction of CO_2 to epoxides in presence of quaternary ammonium salts, the reaction route was assumed to be composed by three consecutive elementary steps: 1) epoxide ring-opening; 2) CO_2 insertion; 3) ring closure of cyclic carbonate. The free energy profile along the reaction coordinate is depicted in Figure 1.

Table 1. Cycloaddition of CO_2 to glycidol (glycidol = 75.4 mmol, $P_{CO_2} = 1.0$ MPa, $t = 1$ h, neat).

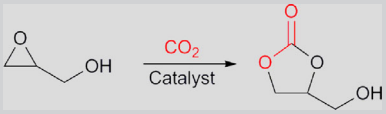

Entry	Catalyst	Catalyst loading [mol%]	Temp. [°C]	Conv.[a] [%]
1	[PPN]Cl	1.0	80	70
2	TBAC	1.0	80	80
3	TBAI	1.0	80	82
4	TBAB	1.0	80	85
5	TBAB	1.0	60	51
6	TBAB	1.0	40	12
7	TBAB	1.0	20	2
8	TBAB	3.0	40	30
9	TBAB	5.0	40	40
10[b]	TBAB	5.0	40	87
11[b]	TBAB	5.0	60	>99
12[c]	TBAB	5.0	40	52
13[b,d]	TBAB	5.0	60	12
14[b,e]	TBAB	5.0	60	4

[a] Determined by ^{1}H NMR using tetrachloroethane as internal standard; the observed selectivity was always >99%. [b] $t = 3$ h. [c] P_{CO_2} = balloon, $t = 24$ h. [d] Methyl glycidyl ether as substrate. [e] PO as substrate.

The contribution of the tetrabutylammonium (TBA) cation was neglected in analogy to previous calculations on the CO_2 coupling promoted by TBAB in presence of a hydrogen-bond activator.[4b]

The reaction starts with the nucleophilic attack of bromide anion to the C3 atom of glycidol, leading to the opening of the oxirane ring through the transition state AB (TS-AB) with a barrier of 12.4 kcal mol^{-1}. The reaction is not regioselective because the nucleophilic attack of bromide anion to the C2 atom proceeds with a slight higher activation barrier (13.7 kcal mol^{-1}, see the Supporting Information for details). In the fol-

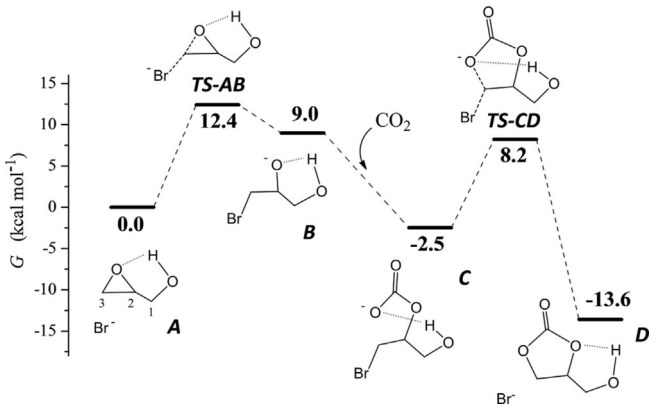

Figure 1. Computed free energy surface for the cycloaddition of glycidol and CO_2 promoted by TBAB. The free energies are given in kcal mol^{-1}.

lowing step, the nucleophilic attack of the alkoxy intermediate B to CO_2 leads to the hemicarbonate intermediate C through a barrier-less reaction pathway in agreement with a previous DFT investigation on similar systems.[19d] The scan of the energy surface corresponding to the approach of the CO_2 to the oxy anion of intermediate B revealed that the energy continues to decrease as the O_{oxy}–C_{CO_2} distance is shortened without any saddle point, supporting that the binding of the CO_2 to intermediate B is a barrier-less process (see the Supporting Information for details). Finally, intermediate C converts into GC through an intramolecular ring-closure reaction that occurs via TS-CD with a barrier of 8.2 kcal mol^{-1}. The total reaction is exergonic by 13.6 kcal mol^{-1} as compared to the reactants.

In this reaction path all intermediates and TSs are involved in an intramolecular hydrogen bond formed between the oxygen atom of the oxirane ring or the oxygen atom of the carboxy group and hydrogen atom of hydroxyl group. To address the importance of the intramolecular hydrogen bonds, we evaluated the Gibbs free energy profile for the same reaction path for PO and methyl glycidyl ether (see Figure 2).

In all cases, the rate-determining step was the nucleophilic attack of the bromide anion to the epoxide ring, the relative activation energy increases in the order glycidol (12.4 kcal mol^{-1}) < methyl glycidyl ether (16.0 kcal mol^{-1}) < PO (17.6 kcal mol^{-1}). Moreover the formation of the first and second intermediates in the case of the methyl glycidyl ether and PO is thermodynamically less favored compared to the case of glycidol. Thus the hydroxyl group is involved in the activation of the epoxide opening and in the stabilization of the two negatively charged intermediates. The trend emerging from our calculations is fully in agreement with the activities experimentally observed for these substrates. Subsequently we explored the influence of the hydrogen bond between the hydroxyl group of a second non-reactive molecule of glycidol and the bromide anion. In this case we found that the epoxide ring-opening steps require overcoming a barrier of 16.2 kcal mol^{-1} (see Supporting Information). This result suggests that the kinetics of the reaction do not overcome the stabilization effect of the second hydrogen bond involving the bromide anion.

With its two hydrogen bond contacts, the oxygen acceptor and hydroxy donor/acceptor, glycidol is capable of forming both intra and intermolecular hydrogen bonds. In the latter case, the mutual hydrogen interactions lead to the formation of dimeric, trimeric, or larger cluster structures. Both theoretical and experimental studies highlighted the peculiar capability of glycidol in chiral self-recognition, that is, the ability of discriminating the same or the opposite enantiomer in the formation of aggregates via intermolecular interactions. Through vibrational circular dichroism and optical rotation measurements, it was established that at low concentration (0.2 M), the equilibrium reaction between the monomer and homochiral dimer is shifted toward the monomer, whereas at higher concentration (3.5 M), the predominant species is the homochiral dimer.[20]

To get more information on the species present in neat liquid, we investigated the concentration dependence of the NMR proton resonances of glycidol. In very dilute solution, the chemical shift of the hydroxyl proton (δ) in $CDCl_3$ is 1.57 ppm. As the concentration of glycidol increases, the resonance is significantly shifted upfield until 3.93 ppm in neat liquid. The drift of the chemical shifts is reported in Figure 3.

The δ of the alcoholic proton of glycidol at 3.27 M is very close to that of neat glycidol (3.61 vs. 3.93 ppm) suggesting that the dimer is the predominant species under the latter condition. Moreover nonlinear least-square analysis of the changes of the proton resonance signal of the hydroxyl group shows a good fit to the monomer–dimer model ($R^2 = 0.983$) with a dimerization constant K_2 of about 0.54 ± 0.10 M^{-1} (see the Supporting Information). Although not elevated, this values reflects the free energy gain when the system switches from an intra- to an inter-molecular hydrogen bond. Theoretical studies shed light on the structure of such a dimer; among the different conformations, the more stable ones are those in which the two monomers form reciprocal hydroxyl–ether hydrogen bonds, leading to eight-membered rings of heavy atoms (8hom, Scheme 2).[21]

Because the hydroxyl group can also act simultaneously as a hydrogen-bond donor and acceptor, stable conformers were also obtained in five-membered heavy atom ring structure and a dangling oxirane ring (5hom, Scheme 2). We used the structures reported in Scheme 2 to remodel the reaction path for the conversion of glycidol to GC, the free energy profiles along the reaction coordinate are reported in Figures 4.

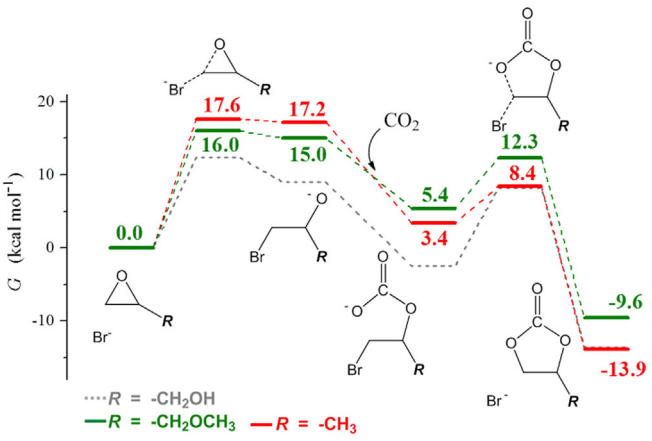

Figure 2. Relative free energy profiles for the cycloaddition of methyl glycidyl ether (green path) and propylene oxide (red path) with CO_2. The reaction profile for glycicol (gray path) is also reported for comparative purposes. The free energies are given in kcal mol^{-1}.

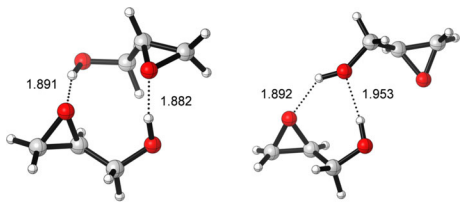

8hom 5hom

Scheme 2. Hydrogen-bond topology of eight-membered (8hom) and five-membered (5hom) ring structures of glycidol dimers.

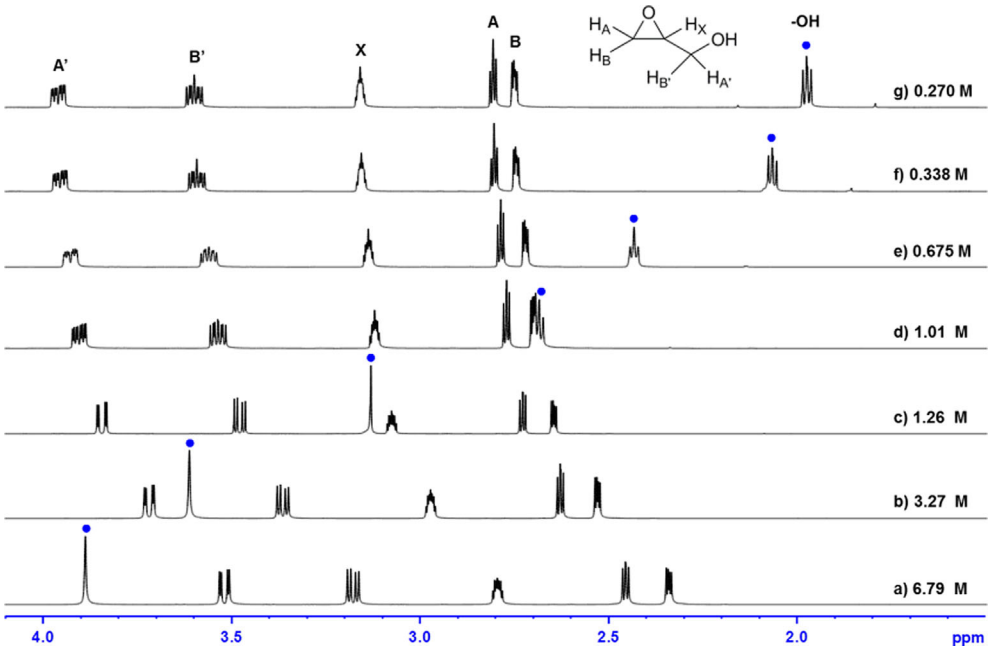

Figure 3. ^{1}H NMR spectra of glycidol at different concentrations ($CDCl_3$; 600 MHz). The symbol "●" indicates the hydroxyl signal.

By comparing the different profiles, it results that the ring opening step is particularly affected by these strong intermolecular hydrogen bonds. As a matter of fact, for both dimers, the nucleophilic attack of the bromide anion to the C3 atom is predicted to occur with a lower activation barrier compared to that found for the monomeric glycidol. In particular, in the case of monomeric glycidol, the ring-opening step requires overcoming a barrier of 12.4 kcal mol^{-1}, whereas in the case of dimeric glycidol featuring the eight-membered heavy atom ring, the activation energy is determined to be 9.8 kcal mol^{-1} and in the case of the dimeric glycidol with the five-membered heavy atom ring, the activation energy is determined to be 8.1 kcal mol^{-1}. It is worth noting that linear correlations between the height of these barriers and the geometric characteristics of the corresponding transition state structures (TS-AB, TS-AB$_{8hom}$, and TS-AB$_{5hom}$, Figure 5) can be found.

In particular, the hydrogen bond distance between the oxy anion and the hydrogen of the hydroxyl group ($d_{O\cdots H}$, Figure 5) becomes shorter (and stronger) in the series TS-AB, TS-AB$_{8hom}$, and TS-AB$_{5hom}$, with a corresponding decrease in the activation barrier. As $d_{O\cdots H}$ decreases, the distance between the oxy anion and C3 atom of the oxirane ring (d_{O-C}, Figure 5) decreases, and the distance between the C3 atom of the oxirane ring and the bromide anion (d_{Br-C}, Figure 5) increases.

Moreover, the alcoholate intermediate B, resulting from this step, is efficiently stabilized by the intermolecular hydrogen present in the dimeric structures. The relative energy of this intermediate follows the same order observed for the activation energies: decreasing from 9.0 kcal mol^{-1} obtained for the intermediate B of monomeric glycerol (Figure 1) to 3.2 kcal mol^{-1} for the same intermediate obtained in the dimer with the eight-membered heavy atom ring (B$_{8hom}$, Figure 4a) until reaching the value of −1.0 kcal mol^{-1} in the case of the dimer with the five-membered heavy atom ring (B$_{5hom}$, Figure 4b). In the last case, the formation of the intermediate is thermodynamically favored.

The ring-closure step is only slightly affected by these intermolecular hydrogen bonds. As matter of fact, the hemicarbonate intermediate formed after the CO_2 addiction has to overcome a barrier of 10.7 kcal mol^{-1} when only an intramolecular hydrogen bond is present (see Figure 1), and a barrier of 9.7 kcal mol^{-1} in case where intermolecular hydrogen bonds are formed (see Figure 4). By comparing the energetics of paths a and b in Figure 4, it can be observed that the barrier of the ring-opening of epoxide in path a is higher than that in path b by 1.7 kcal mol^{-1}, and the barrier of the ring closure of cyclic carbonate is the same for the both paths, which implies that the two intermolecular hydrogen-bond networks in the dimers of glycidol are equally effective in reducing the barriers for nucleophilic attack of the bromide anion to the epoxide ring.

Owing to the unique behavior of glycidol in forming intermolecular hydrogen bonds, we envisaged the possibility to use this hydrogen-bond donor molecule as catalyst component, in combination with a nuclophile, for the conversion of other epoxides into the corresponding cyclic carbonates. Accordingly we used the binary system glycidol/TBAB as organocatalyst, for the conversion of PO to propylene carbonate (PC) as benchmark. The results reported in Table 2 clearly show that under the same reaction conditions the binary system is sensibly more active (entry 4, Table 2) compared to the use of TBAB alone (entry 5, Table 2).

It is worth noting that under very mild conditions (T = 60 °C, P_{CO_2} = 1.0 MPa) PO can be converted to PC in very good yield (entry 7, Table 2). Thus, under these reaction conditions, glycidol activates the PO towards the nucleophilic attack of the

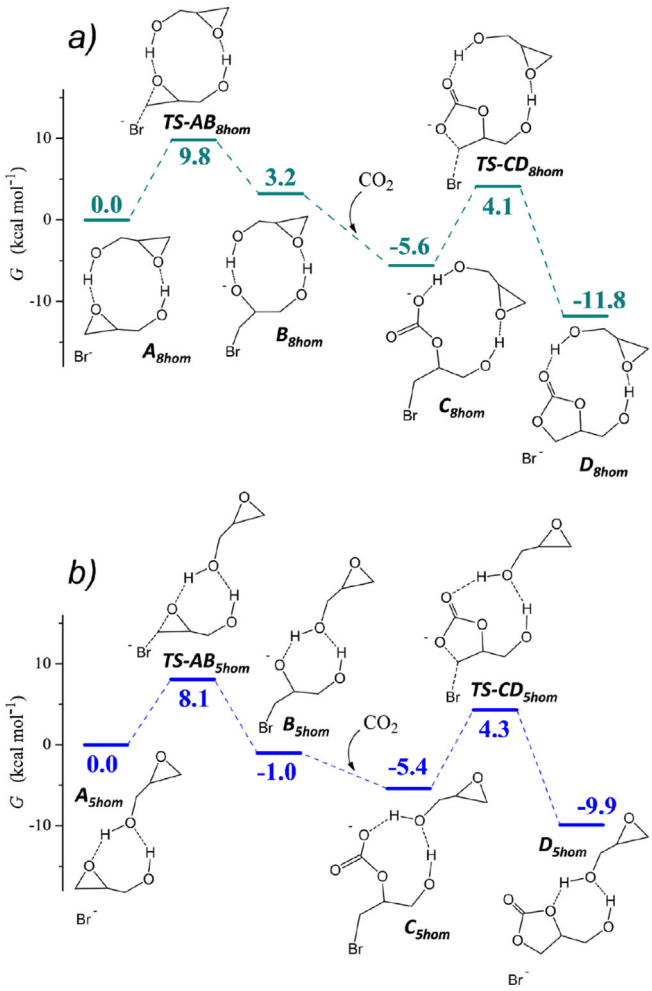

Figure 4. Relative free energy profiles for the cycloaddition of glycicol computed for the dimers of glycidol featuring the (a) eight-membered heavy atom ring (8hom) and (b) five-membered heavy atom ring (5hom). The free energies are given in kcal mol^{-1}.

bromide and convert itself to GC, playing the double role of organocatalyst and substrate and rendering the recovery of the catalyst superfluous owing to the low catalyst loading and to the close chemical and physical properties of the main product and GC.

Indeed, under these reaction conditions one can expect that glycidol is firstly converted to GC and thus the true organocatalyst is the latter compound that also can act as hydrogen-bond donor. As a matter of fact, the binary system GC/TBAB give the same results in term of conversion and selectivity than the binary system glycidol/TBAB (compare entries 7 and 9, Table 2) supporting this hypothesis.

Table 2. Cycloaddition of CO_2 to propylene oxide in the presence of glycidol and TBAB as catalytic system (PO = 71.5 mmol, P_{CO_2} = 1.0 MPa, t = 24 h, neat).

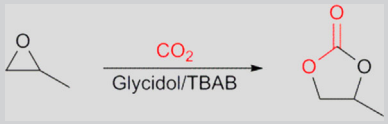

Entry	Glycidol [mol%]	TBAB [mol%]	Temp. [°C]	Yield[a] [%]
1	1	1	50	15
2	1	1	60	40
3	1	1	70	66
4	1	1	80	83
5	–	1	80	30
3	3	3	60	63
7	5	5	60	84
8	–	5	60	16
9[b]	5	5	60	85

[a] Isolated yield, the observed selectivity was always >99%. [b] GC in place of glycidol.

Finally, to test the activity of this new binary catalytic system to a wider family of substrates, we performed, under mild reaction conditions, the cycloaddition of CO_2 to a series of oxiranes (Table 3). All the substrates are converted into the corresponding carbonates in high to excellent yields. In particular, in the case of epichlorohydrin the presence of the electron withdrawing chlorine atom on the epoxy ring is beneficial giving the highest conversion observed. In addition the more challenging internal epoxide cyclohexeneoxide is also converted in moderate yield that well compare with the most active organocatalysts.[2]

Conclusions

A simple and efficient route to obtain glycerol carbonate (GC) was developed by coupling of glycidol with CO_2. Owing to the formation of hydrogen bonds between the glycidol molecules, this substrate behaves uniquely, playing the double role of

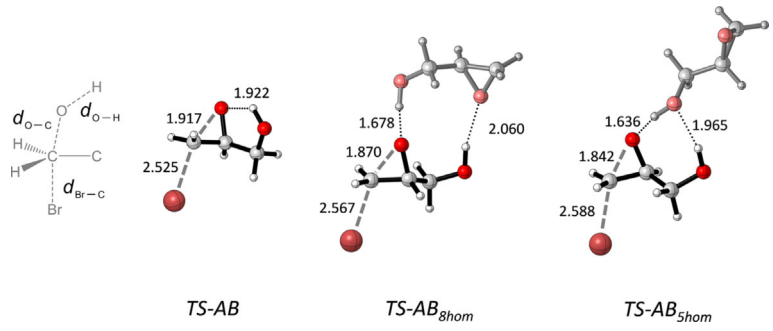

Figure 5. Transition state structures for the ring-opening step for monomer (TS-AB) and dimer of glicidol (TS-AB$_{5hom}$ and TS-AB$_{8hom}$). Distances are given in Å.

Table 3. Cycloaddition of CO_2 to various epoxides in the presence of glycidol and TBAB as catalytic system (epoxide = 71.5 mmol, glycidol = 1 mol%, TBAB = 1 mol%, P_{CO_2} = 1.0 MPa, T = 60 °C, t = 24 h, neat).

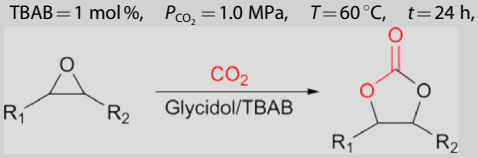

Entry	Epoxide	Conversion[a] [%]
1[b]	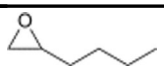	26 (12)
2	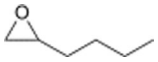	31 (21)
3[c]	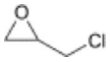	83 (65)
4[d]	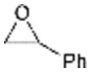	85 (45)
5	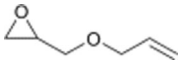	57 (42)
6[e]	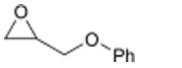	76 (66)
7[d,e]		19 (6)

[a] Determined by ^{1}H NMR using mesitylene as internal standard, the observed selectivity was always >99%. The values in brackets are the conversions in absence of glycidol. [b] P_{CO_2} = balloon. [c] Glycidol = 5 mol%, TBAB = 5 mol%, t = 3 h. [d] Glycidol = 5 mol%, TBAB = 5 mol%. [e] Methyl ethyl ketone (MEK) = 10 mL.

substrate and catalyst in this reaction, allowing the synthesis of GC under metal-free, solvent-free, and rather mild reaction conditions (T = 60–80 °C, P_{CO_2} = 0.1–1 MPa) and short times (t = 1–3 h).

The mechanism of the reaction was studied using density functional theory (DFT). The nucleophilic attack by the bromide anion was revealed to be the rate determining step. The hydroxyl group of glycerol, acting as a hydrogen-bond donor, serves to activate the epoxide for the ring opening and to stabilize the two negatively charged intermediates, and is thus essential for reaction rate. Analysis of the hydrogen-bond network revealed that the intermolecular hydrogen-bond interactions are particularly effective in facilitating the reaction pathway for the conversion of glycerol to GC. To extend the applicability of this substrate in the field of the CO_2 fixation reaction, we explored the possibility of using glycerol as a co-catalyst for the TBAB-catalyzed cycloaddition. Actually, the binary system glycidol/TBAB can act as efficient organocatalyst for the conversion of diverse epoxides into the corresponding cyclic carbonates in high-to-excellent yields under very mild conditions (T = 60–80 °C, P_{CO_2} = 0.1–1 MPa). Finally the low catalyst loading and the fact that the glycidol is also converted to the corresponding carbonate render the recovery of the catalyst superfluous for most applications making this catalytic system sustainable from both the environmental and economical point of views.

Experimental Section

Materials and methods

Glycidol (Sigma–Aldrich) was distilled under reduced pressure prior to use. All other reagents were used as-received (Sigma–Aldrich or TCI Europe). Deuterated solvents were purchased from Euriso-Top or Sigma–Aldrich and used as received. NMR spectra were collected on Bruker Avance spectrometers (600, 400, 300, or 250 MHz for ^{1}H NMR): the chemical shifts were referenced to tetramethylsilane (TMS) as external reference, using the residual protio signal of the deuterated solvents.

General procedure for CO_2/glycidol coupling to glycerol carbonate

A 60 mL stainless steel pressure reactor equipped with a magnetic stirring bar was charged with TBAB (0.754 mmol, 0.2430 g). Three cycles of pressurization-depressurization were carried out and glycidol (5.0 mL, 75.4 mmol) was introduced in the reactor. The reaction mixture was pressurized with CO_2 at 1.0 MPa and stirred at 80 °C for 1 h. The reactor was cooled with ice, the CO_2 released, tetrachloroethane (0.8 mL, 7.54 mmol) was added as an internal standard and the mixture was analyzed by ^{1}H NMR spectroscopy using $CDCl_3$ as solvent. Conversion: 85%.

General procedure for CO_2/propylene oxide coupling to propylene carbonate

A 60 mL stainless steel pressure reactor equipped with a magnetic stirring bar was charged with TBAB (0.715 mmol, 0.2303 g) and glycidol (47 μL, 0.715 mmol). Three cycles of pressurization–depressurization were carried out and propylene oxide (5.0 mL, 71.4 mmol) was introduced in the reactor. The reaction mixture was pressurized with CO_2 at 1.0 MPa and stirred at 80 °C for 24 h. The reactor was cooled with ice, the CO_2 released. Unreacted epoxide was removed under vacuum. The residue was dissolved in methylene chloride, filtered over silica and the solvent removed under vacuum. Isolated yield: 85%.

Typical procedure for CO_2/epoxide coupling to the corresponding cyclic carbonate

The procedure for 1,2-epoxyhexane is as reported: A 60 mL stainless steel pressure reactor equipped with a magnetic stirring bar was charged with TBAB (3.57 mmol, 1.15 g) and glycidol (237 μL, 3.57 mmol). Three cycles of pressurization–depressurization were carried out and 1,2-epoxyhexane (8.6 mL, 71.4 mmol) was introduced in the reactor. The reaction mixture was pressurized with CO_2 at 1.0 MPa and stirred at 60 °C for 24 h. The reactor was cooled with ice, the CO_2 released, mesitylene (1.0 mL, 7.14 mmol) was added as an internal standard, and the mixture was analyzed by ^{1}H NMR spectroscopy using $CDCl_3$ as solvent. Conversion: 93%. For other epoxides a similar procedure was employed.

Typical procedure for CO_2/epoxide coupling to the corresponding cyclic carbonate at low pressure

The procedure for 1,2-epoxyhexane is as reported: A 50 mL three-neck round-bottom flask equipped with a magnetic stirring bar and a condenser was charged with TBAB (3.57 mmol, 1.15 g) and glycidol (237 μL, 3.57 mmol). The flask was flushed with CO_2 and

1,2-epoxyhexane (8.6 mL, 71.4 mmol) was introduced in the reactor. The apparatus was connected to a balloon filled with CO_2 and the reaction mixture stirred at 60 °C for 24 h. The reactor was cooled with ice, the CO_2 released, mesitylene (1.0 mL, 7.14 mmol) was added as an internal standard and the mixture was analyzed by ^{1}H NMR spectroscopy using $CDCl_3$ as solvent. Conversion: 56%. For other epoxides a similar procedure was employed.

Computational details

All computations were carried out using the Becke's three-parameter hybrid exchange functional in combination with the gradient-corrected correlation functional of Lee, Yang, and Parr (B3LYP) by using the GAUSSIAN 09 program packages.[22] The basis set employed was 6-31 + g(d) for all atoms. Stationary point geometries were characterized as local minimum on the potential energy surfaces. The absence of imaginary frequency verified that structures were true minima at their respective levels of theory. The structure of transition state were located by applying Schlegel's synchronous-transit-guided quasi-Newton (QST2) method as implemented in GAUSSIAN 09. The transition states were verified with frequency calculations to ensure they were first-order saddle points with only one negative eigenvalue. The free energy differences reported in Figures 1, 2, and 4 are in gas phase, the sum of the free energies of the CO_2 and the adduct between the bromide anion and epoxide is taken as zero energy. Cartesian coordinates of all DFT-optimized structures are available on request. Structures were visualized by the CYLview program.[23]

Acknowledgements

Financial support is acknowledged from the Ministero dell'Istruzione dell'Università e della Ricerca (MIUR, Roma, Italy for FARB 2015) and the SPRING cluster (REBIOCHEM research project CTN01_00063_49393). The Centro di Tecnologie Integrate per la Salute (Project PONa3_00138) for the 600 MHz NMR instrumental time is acknowledged. The authors are also grateful to Dr. Patrizia Oliva and Dr. Patrizia Iannece from University of Salerno for technical assistance.

Keywords: carbon dioxide · cycloaddition · density functional theory · epoxide · hydrogen bond

[1] a) C. Martín, G. Fiorani, A. W. Kleij, *ACS Catal.* **2015**, *5*, 1353 – 1370; b) J. W. Comerford, I. D. V. Ingram, M. North, X. Wu, *Green Chem.* **2015**, *17*, 1966 – 1987; c) M. Cokoja, C. Bruckmeier, B. Rieger, W. A. Herrmann, F. E. Kühn, *Angew. Chem. Int. Ed.* **2011**, *50*, 8510 – 8537; *Angew. Chem.* **2011**, *123*, 8662 – 8690; d) A. Decortes, A. M. Castilla, A. W. Kleij, *Angew. Chem. Int. Ed.* **2010**, *49*, 9822 – 9837; *Angew. Chem.* **2010**, *122*, 10016 – 10032; e) P.-Z. Li, X.-J. Wang, J. Liu, J. S. Lim, R. Zou, Y. Zhao, *JACS* **2016**, *138*, 2142 – 2145.

[2] a) X. F. Liu, Q. W. Song, S. Zhang, L. N. He, *Catal. Today* **2016**, *263*, 69 – 74; b) M. Cokoja, M. E. Wilhelm, M. H. Anthofer, W. A. Hermann, F. E. Kühn, *ChemSusChem* **2015**, *8*, 2436 – 2454; c) G. Fiorani, W. Guo, A. W. Kleij, *Green Chem.* **2015**, *17*, 1375 – 1389.

[3] a) J. Ma, J. Song, H. Liu, Z. Zhang, T. Jiang, H. Fan, B. Han, *Green Chem.* **2012**, *14*, 1743 – 1748; b) T. Werner, N. Tenhumberg, H. Büttner, *ChemCatChem* **2014**, *6*, 3493 – 3500; c) M. E. Wilhelm, M. H. Anthofer, M. Cokoja, I. I. Markovitis, W. A. Hermann, F. E. Kühn, *ChemSusChem* **2014**, *7*, 1357 – 1360; d) S. Gennen, M. Alves, R. Méreau, T. Tassaing, B. Gilbert, C. Detrembleur, C. Jerome, B. Grignard, *ChemSusChem* **2015**, *8*, 1845 – 1849; e) H. Büttner, J. Steinbauer, T. Werner, *ChemSusChem* **2015**, *8*, 2655 – 2669.

[4] a) J. W. Huang, M. Shi, *J. Org. Chem.* **2003**, *68*, 6705 – 6709; b) C. J. Whiteoak, A. Nova, E. Maseras, A. W. Kleij, *ChemSusChem* **2012**, *5*, 2032 – 2038; c) S. Sopeña, G. Fiorani, C. Martin, A. W. Kleij, *ChemSusChem* **2015**, *8*, 3248 – 3254; d) M. Alves, B. Grignard, S. Gennen, R. Mereau, C. Detrembleur, C. Jerome, T. Tassaing, *Catal. Sci. Technol.* **2015**, *5*, 4636 – 4643; e) M. Alves, B. Grignard, S. Gennen, C. Detrembleur, C. Jerome, T. Tassaing, *RSC Adv.* **2015**, *5*, 53629 – 53636; f) L. M. Rodríguez, J. O. Garmilla, A. W. Kleij, *ChemSusChem* **2016**, *9*, 749 – 755.

[5] a) L. Han, H. J. Choi, B. Liu, D.-W. Park, *Green Chem.* **2011**, *13*, 1023 – 1028; b) J. Tharun, G. Mathai, A. C. Kathalikattil, R. Roshan, J.-Y. Kwak, D.-W. Park, *Green Chem.* **2013**, *15*, 1673 – 1677.

[6] A. M. Hardman-Baldwin, A. E. Mattson, *ChemSusChem* **2014**, *7*, 3275 – 3278.

[7] a) J. Sun, J. Wang, W. Cheng, J. Zhang, X. Li, S. Zhang, Y. She, *Green Chem.* **2012**, *14*, 654 – 660; b) J. Tharun, Y. Hwang, R. Roshan, A. C. Kathalikattil, D.-W. Park, T. Tassaing, *Catal. Sci. Technol.* **2012**, *5*, 1674 – 1680; c) C. Jing-Xiana, J. Bia, D. Wei-Lia, D. Sen-Lina, C. Liu-Rena, C. Zong-Jiea, L. Sheng-Liana, L. Xu-Biaoa, T. Xin-Mana, A. Chak-Tong, *Appl. Catal. A* **2014**, *484*, 26 – 32.

[8] a) S. Liang, H. Liu, T. Jiang, J. Song, G. Yang, B. Han, *Chem. Commun.* **2011**, *47*, 2131 – 2133; b) J. Sun, W. Cheng, Z. Yang, J. Wang, T. Xu, J. Xin, S. Zhang, *Green Chem.* **2014**, *16*, 3071 – 3078.

[9] J. L. Song, Z. F. Zhang, B. X. Han, S. Q. Hu, W. J. Li, Y. Xie, *Green Chem.* **2008**, *10*, 1337 – 1341.

[10] a) Z. F. Yang, J. Sun, W. G. Cheng, J. Q. Wang, Q. Li, S. J. Zhang, *Catal. Commun.* **2014**, *44*, 6 – 9; b) T. Werner, N. Tenhumberg, *J. CO2 Utilization* **2014**, *7*, 39 – 45; c) L. Wang, G. Zhang, K. Kodama, T. Hirose, *Green Chem.* **2016**, *18*, 1229 – 1233; d) Z. Guo, X. Cai, J. Xie, X. Wang, Y. Zhou, J. Wang, *ACS Appl. Mater. Interfaces* **2016**, *8*, 12812 – 12821.

[11] a) D.-H. Lan, F.-M. Yang, S.-L. Luo, C.-T. Au, S.-F. Yin, *Carbon* **2014**, *73*, 351 – 360; b) W.-H. Zhang, P.-P. He, S. Wu, J. Xu, Y. Li, G. Zhang, X.-Y. Wei, *Appl. Catal. A* **2016**, *509*, 111 – 117.

[12] a) M. Pagliaro, R. Ciriminna, H. Kimura, M. Rossi, C. D. Pina, *Angew. Chem. Int. Ed.* **2007**, *46*, 4434 – 4440; *Angew. Chem.* **2007**, *119*, 4516 – 4522; b) J. J. Bozell, G. R. Petersen, *Green Chem.* **2010**, *12*, 539 – 554; c) C. Simões, S. Baranton, C. Coutanceau, *ChemSusChem* **2012**, *5*, 2106 – 2124; d) J. I. García, H. Garcia-Marín, E. Pires, *Green Chem.* **2014**, *16*, 1007 – 1033; e) M. Sutter, E. Da Silva, N. Duguet, Y. Raoul, E. Métay, M. Lemaire, *Chem. Rev.* **2015**, *115*, 8609 – 8651.

[13] M. O. Sonnati, S. Amigoni, E. P. T. de Givenchy, T. Darmanin, O. Choulet, F. Guittard, *Green Chem.* **2013**, *15*, 283 – 306.

[14] a) J. R. Ochoa-Gómez, O. Gómez-Jiménez-Aberasturi, C. Ramírez-López, M. Belsué, *Org. Process Res. Dev.* **2012**, *16*, 389 – 399; b) W. Jacquemin in *Encyclopedia of Chemical Processing and Design, Vol. 20* (Eds.: J. J. McKetta, W. A. Cunningham), Marcel Decker, New York, **1984**, pp. 177 – 201; c) C. Vieville, J. W. Yoo, S. Pelet, Z. Mouloungui, *Catal. Lett.* **1998**, *56*, 245; d) Y. Patel, J. George, S. M. Pillai, P. Munshi, *Green Chem.* **2009**, *11*, 1056; e) A. Takagaki, K. Iwatami, S. Nishimura, K. Ebitani, *Green Chem.* **2010**, *12*, 578 – 581.

[15] a) M. Aresta, A. Di Benedetto, F. Nocito, C. Pastore, *J. Mol. Catal. A* **2006**, *257*, 149 – 153; b) J. George, Y. Patel, S. M. Pillai, P. Munshi, *J. Mol. Catal. A* **2009**, *304*, 1 – 7.

[16] a) Q. Li, W. Zhang, N. Zhao, W. Wei, Y. Sun, *Catal. Today* **2006**, *115*, 111 – 116; b) M. Aresta, A. Dibenedetto, F. Nocito, C. Ferragina, *J. Catal.* **2009**, *268*, 106 – 114; c) A. Dibenedetto, A. Angelini, M. Aresta, J. Ethiraj, C. Fragale, F. Nocito, *Tetrahedron* **2011**, *67*, 1308 – 1313.

[17] a) M. North, C. Young, *Catal. Sci. Technol.* **2011**, *1*, 93 – 99; b) C. J. Whiteoak, E. Martin, M. M. Belmonte, J. Bene *t*Buchholz, A. W. Kleij, *Adv. Synth. Catal.* **2012**, 354, 469 – 476; c) C. J. Whiteoak, N. Kielland, V. Laserna, E. C. Escudero-Adán, E. Martin, A. W. Kleij, *J. Am. Chem. Soc.* **2013**, *135*, 1228 – 1231; d) C. J. Whiteoak, N. Kielland, V. Laserna, F. Castro-Gómez, E. Martin, E. C. Escudero-Adán, C. Bo, A. W. Kleij, *Chem. Eur. J.* **2014**, *20*, 2264 – 2275; e) J. A. Castro-Osma, M. North, X. Wu, *Chem. Eur. J.* **2014**, *20*, 15005 – 15008; f) J. Martínez, J. A. Castro-Osma, A. Earlam, C. Alonso-Moreno, A. Otero, A. Lara-Sánchez, M. North, A. Rodrìguez-Diéguez, *Chem. Eur. J.* **2015**, *21*, 9850 – 9862; g) A. Buonerba, A. De Nisi, A. Grassi, S. Milione, C. Capacchione, S. Vagin, B. Rieger, *Catal. Sci. Technol.* **2015**, *5*, 118 – 112; h) A. Buonerba, F. Della Monica, A. De Nisi, E. Luciano, S. Milione, A. Grassi, C. Capacchione, B. Rieger, *Faraday Discuss.* **2015**, *183*,

83 – 95; i) F. Della Monica, S. V. C. Vummaleti, A. Buonerba, A. De Nisi, M. Monari, S. Milione, A. Grassi, L. Cavallo, C. Capacchione, *Adv. Synth. Catal.*, **2016**, *358*, 3231 – 3243; j) J. Rintjema, R. Epping, G. Fiorani, E. Martín, E. C. Escudero-Adán, A. W. Kleij, *Angew. Chem. Int. Ed.* **2016**, *55*, 3972 – 3976; *Angew. Chem.* **2016**, *128*, 4040 – 4044.

[18] D. Cespi, R. Cucciniello, M. Ricciardi, C. Capacchione, I. Vassura, F. Passarini, A. Proto, *Green Chem*. **2016**, *18*, 4559 – 4570.

[19] a) V. Caló, A. Nacci, A. Monopoli, A. Fanizzi, *Org. Lett.* **2002**, *4*, 2561 – 2563; b) J.-Q. Wang, K. Dong, W.-G. Cheng, J. Sun, S.-J. Zhang, *Catal. Sci. Technol.* **2012**, *2*, 1480 – 1484; c) T. Ema, K. Fukuhara, T. Sakai, M. Ohbo, F.-Q. Bai, J. Hasegawa, *Catal. Sci. Technol.* **2015**, *5*, 2314 – 2321; d) C. C. Rocha, T. Onfroy, J. Pilmé, A. Denicourt-Nowicki, A. Roucoux, F. Launay, *J. Catal.* **2016**, *333*, 29 – 39.

[20] G. Yang, Y. Xu, *Phys. Chem. Chem. Phys.* **2008**, *10*, 6787 – 6795.

[21] a) N. Borho, T. Häber, M. A. Suhm, *Phys. Chem. Chem. Phys.* **2001**, *3*, 1945 – 1948; b) N. Borho, M. A. Suhm, *Phys. Chem. Chem. Phys.* **2002**, *4*, 2721 – 2732.

[22] Gaussian 09 (Revision A.02), M. J. Frisch, G. W. Trucks, H. B. Schlegel, G. E. Scuseria, M. A. Robb, J. R. Cheeseman, G. Scalmani, V. Barone, B. Mennucci, G. A. Petersson, H. Nakatsuji, M. Caricato, X. Li, H. P. Hratchian, A. F. Izmaylov, J. Bloino, G. Zheng, J. L. Sonnenberg, M. Hada, M. Ehara, K. Toyota, R. Fukuda, J. Hasegawa, M. Ishida, T. Nakajima, Y. Honda, O. Kitao, H. Nakai, T. Vreven, J. A. Montgomery, Jr., J. E. Peralta, F. Ogliaro, M. Bearpark, J. J. Heyd, E. Brothers, K. N. Kudin, V. N. Staroverov, R. Kobayashi, J. Normand, K. Raghavachari, A. Rendell, J. C. Burant, S. S. Iyengar, J. Tomasi, M. Cossi, N. Rega, J. M. Millam, M. Klene, J. E. Knox, J. B. Cross, V. Bakken, C. Adamo, J. Jaramillo, R. Gomperts, R. E. Stratmann, O. Yazyev, A. J. Austin, R. Cammi, C. Pomelli, J. W. Ochterski, R. L. Martin, K. Morokuma, V. G. Zakrzewski, G. A. Voth, P. Salvador, J. J. Dannenberg, S. Dapprich, A. D. Daniels, O. Farkas, J. B. Foresman, J. V. Ortiz, J. Cioslowski, D. J. Fox, Gaussian, Inc.: Wallingford, CT, **2009**.

[23] C. Y. Legault CYLview, v1.0b, Université de Sherbrooke, **2009**; http://www.cylview.org.

Received: August 22, 2016
Revised: October 7, 2016
Published online on ■■ ■■, 0000

Double duty: Glycydol is efficiently converted to glycerol carbonate by coupling with CO_2 in the presence of tetrabutylammonium bromide under metal-free, solvent free reaction conditions. Density functional theory calculations supported by ^1H NMR experiments reveal that the unique behavior of this substrate is a result of the formation of intermolecular hydrogen bonds, activating this molecule to nucleophilic attack.

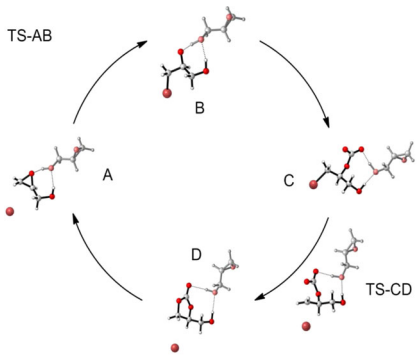

F. Della Monica, A. Buonerba, A. Grassi, C. Capacchione, S. Milione*

■■ – ■■

Glycidol: an Hydroxyl-Containing Epoxide Playing the Double Role of Substrate and Catalyst for CO_2 Cycloaddition Reactions

These are not the final page numbers! ↗↗